Ultrasound Sensor Array for Robust Location

José N. Vieira[1], Sérgio I. Lopes[2], Carlos A. C. Bastos[1] and Pedro N. Fonseca[1]

[1] Departamento de Electrónica, Telecomunicações e Informática / IEETA
Universidade de Aveiro 3810-193 Aveiro, Portugal

Abstract. In this paper we present a system for localizing a team of soccer robots using ultrasound. The proposed system uses chirp signals to obtain a better signal to noise ratio with good time resolution and improved interference immunity. An array of four ultrasonic sensors is used to obtain spatial diversity and reduce the localization error. An efficient DSP algorithm for base-band conversion and decimation of the received pulses is also presented. The proposed system based on the TI DSP 2812 is very efficient and allows the localization of the robots up to 8 meters with an angular error with a maximum standard deviation of 2°.

1 Introduction

Ultrasonic Sensors (USS) systems are widely used in robotics for obstacle localization and mutual robot localization [1], [2]. Most of the commercial available ultrasonic systems use a sinusoidal pulse to measure the Time of Flight (TOF). Usually these systems perform badly in the presence of interferences and various authors have presented more complex alternatives using different types of modulation of the emitted ultrasonic pulse [3] and [4].

This paper describes an ongoing work to build a localization system, using USS for a team of soccer robots. The main achievements of this work are the efficient implementation of the baseband converter of the received bandpass chirp pulses, and the array with four sensors using an algorithm that integrates several measurements in time and space resulting in a small error for distances up to 8 meters.

The specifications for this system require that it should be able to locate each of the mobile robots (MR) with an accuracy better than ± 0.5 meters for distances up to 8 meters.

Since the goalkeeper has reduced mobility and its position can easily be determined by the vision location system, all the positions of the other robots are referenced to its position. The goalkeeper has an array of four aligned sensors at 20cm from each other as can be seen in figure 1. Each field MR has four emitters and receivers equally spaced over a circle and working like a transponder. The measurement of the position of each MR is performed in the following way: the goalkeepere emits an ultrasound start signal, then each MR answer after $n \times 50ms$ where n is the MR number ID. This guarantees the time interleaving of the answers. The goalkeeper evaluates the distance to each robot n by

$$d_n = c(T_n - n \times 50ms) = cTOF_n, \tag{1}$$

N. Vieira J., I. Lopes S., A. C. Bastos C. and N. Fonseca P. (2007).
Ultrasound Sensor Array for Robust Location.
In *Proceedings of the 3rd International Workshop on Multi-Agent Robotic Systems*, pages 84-93
Copyright © SciTePress

where T is the total measured time between the start signal and the received signal from the MR, TOF is the time of flight and c the sound speed.

2 Localization System

A previous version of the localization system had only two receivers located 20cm apart. This system was very sensible to small errors in the TOF measurements leading to an unusable system [5]. We solved this problem by acting on various aspects of the system. Firstly, we increased the applied voltage to the transmitter from 8 to 16Volts. Then we built an array with four aligned sensors spaced 20cm from each other to obtain spatial diversity and as a consequence increased stability in position evaluation. Finally, we improved the algorithm that evaluates the (x_m, y_m) by integrating several sets of four measures T_i to get an extra gain in the position stability.

The digital signal processing of the localization system is carried out by a DSP2812. If all the digital signal processing was performed at the sampling frequency of 160kHz, the DSP 2812 would not have enough processing power to calculate the TOF for the four channels. In order to circumvent this limitation, we implemented a baseband converter that outputs the decimated quadrature and phase components of the input signal. The baseband converter was implemented directly in DSP2812 assembly language and it uses about 50% of the available DSP processing power. The baseband converter reduces the sampling frequency by a factor of 32, from 160kHz to 5kHz. The processing of the converter output is much less demanding on the processing power and was implemented in C.

2.1 Time of Flight Measurement

The transmitted chirp pulse is generated by sampling the signal

$$c(t) = h(t)\cos\left(\omega_1 t + \beta t^2\right), \qquad t \in [0 \dots T],$$

with $\beta = (\omega_2 - \omega_1)/(2T)$, where ω_1 and ω_2 are the initial and final frequencies of the chirp, T is the duration of the pulse and $h(t)$ is a Hamming window. The window $h(t)$ is used to reduce the side lobes that appear on the autocorrelation of the chirp. The carrier frequency is defined as $\omega_c = (\omega_1 + \omega_2)/2$.

Figure 2 shows the chirp autocorrelation with and without the Hamming window. The reduction of the sidelobes is important to avoid false peak detection.

Baseband converter For bandpass signals, the Nyquist theorem states that a signal has to be sampled at a frequency not less than twice the bandwidth of the signal. Since the bandwidth of $c(t)$ is typically 2kHz (in our system) it is possible to reduce the sampling frequency to a much lower value (5kHz) by performing a bandpass to lowpass transformation (see figure 3). This technique is well known and widely used on radar and ultrasound sensing [6]. Several methods are available to perform this conversion e.g. [7].

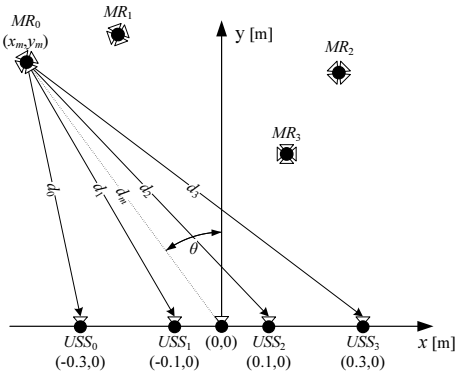

Fig. 1. Locating the MR with the four sensor USS$_i$ array and the goalkeeper emitter (located at the origin).

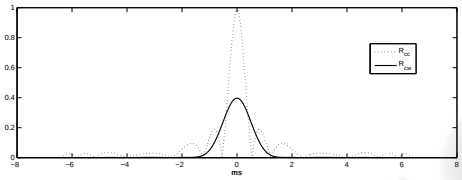

Fig. 2. Cross correlation of the chirp (dotted line) and the chirp multiplied by a Hamming window (solid line).

In this system we used low cost ultrasonic transducers from Murata that have a large aperture (MA40S4R and MA40S4S), essential to cover all the field. Their bandpass frequency response is centered at 40kHz with a useful bandwidth of 2kHz. The emitted pulses are chirps ranging from 39 to 41kHz with a duration of 6.4ms. As the baseband converted chirp has a bandwidth of only 1kHz the signal is decimated by 32 resulting in a sampling frequency of 5kHz which is enough to represent the signal.

Figure 4 shows the structured of the baseband converter as implemented in this work. We managed to simplify the calculations needed to perform the baseband conversion by specifying an integer relation between the sampling frequency and the carrier frequency and by integrating the modulators within the filters structure. The filter was implemented using a polyphase decomposition [8]. In order to calculate both outputs x_i and x_q, the system only has to perform N/D product-accumulation operations for each input signal sample, where N is the number of coefficients of the filter and D the decimation factor. As the filter $H(z)$ has $N = 256$ coefficients and the decimation factor is $D = 32$ the system only has to perform 8 mult/adds for each filter phase $H_k(z)$, with

$$H(z) = \sum_{k=0}^{D-1} z^{-k} H_k(z^D).$$

The first simplification on the system is achieved by making the sampling frequency four times greater than the carrier frequency (40kHz). This results in the following sequences at the output of the modulators

$$\cos\left(2\pi\frac{f_c}{f_s}n\right) = \{1, 0, -1, 0, \ldots\}$$
$$\sin\left(2\pi\frac{f_c}{f_s}n\right) = \{0, 1, 0, -1, \ldots\}$$

with $n \in \mathbb{Z}$. After the multipliers we have the following signals

$$x(n)\cos\left(2\pi\frac{f_c}{f_s}n\right) = \{x(0), 0, -x(2), 0, \ldots\} \tag{2}$$
$$x(n)\sin\left(2\pi\frac{f_c}{f_s}n\right) = \{0, x(1), 0, -x(3), \ldots\}\,. \tag{3}$$

We can see that each lowpass filter only has to process half the samples because the other half is zero. Using a polyphase decomposition of the lowpass filters we can move the decimator from the output of the filters to within the filter structure.

Finally, as the signals at the input of the filters have half of the samples equal to zero and noting that both lowpass filters are equal, we can add the two signals from (2) to obtain the signal

$$x(n)\left[\cos(\omega_c n) + \sin(\omega_c n)\right] = \\ = \{x(0), x(1), -x(2), -x(3), \ldots\}\,.$$

If the decimation factor is even we can decompose the decimators in the polyphase filter structure as shown in figure 4 where the input signal is separated in two different phases. The phase corresponding to the signal from (2) will be processed by the even filter phases, while the signal from (3) will be processed by the odd filter phases. At the output of the filter we have two summations, one for each filter phase obtaining the two outputs, the in-phase x_i and the quadrature x_q.

This compact structure allowed the optimization of the assembly code by minimizing the need of pointer manipulation.

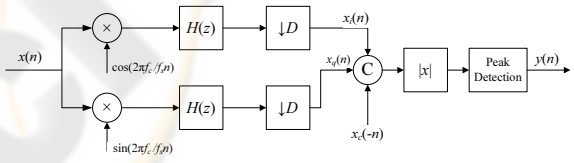

Fig. 3. Block diagram of the base band converter.

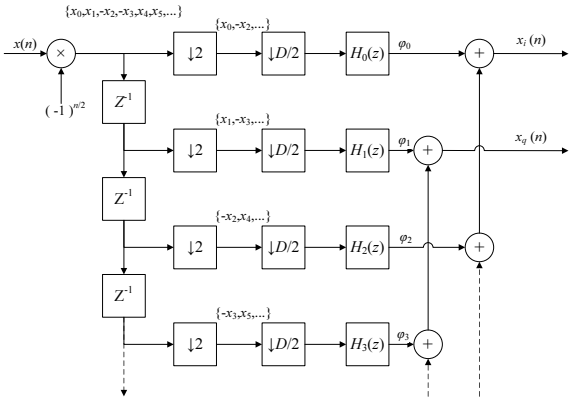

Fig. 4. Equivalent baseband converter implemented in an efficient way.

Envelope Interpolation The envelope of the correlator output signal needs to be computed in order to determine the time position of its peak. Since the sampling period of the signal is $1/5000 = 0.2$ms, the system cannot directly discriminate time differences smaller than this limit. In order to improve the time resolution of the peak detection we followed the [7] approach and interpolated the envelope of the decimated signal using quadratic interpolation.

It is well known that there is a unique quadratic function that passes through any three points. Moreover, the interpolating polynomial of degree $N-1$ through the points $y_1 = y(t_1), y_2 = y(t_2), y_3 = y(t_3)$ is given explicitly by Lagrange's classical formula, presented in equation (4) for $N = 3$,

$$\begin{aligned} y(t) =& \frac{(t-t_2)(t-t_3)}{(t_1-t_2)(t_1-t_3)} y_1 + \\ &+ \frac{(t-t_1)(t-t_3)}{(t_2-t_1)(t_2-t_3)} y_2 + \\ &+ \frac{(t-t_1)(t-t_2)}{(t_3-t_1)(t_3-t_2)} y_3. \end{aligned} \tag{4}$$

From the previous equation we can get the maximum of $y(t)$ by finding the value t that nulls the first derivative of $y(t)$. This value is given by

$$t = \frac{t_3(k_1+k_2) + t_2(k_1+k_3) + t_1(k_2+k_3)}{2(k_1+k_2+k_3)}$$

where

$$k_1 = \frac{y_1}{(t_1-t_2)(t_1-t_3)}$$

$$k_2 = \frac{y_2}{(t_2-t_1)(t_2-t_3)}$$

$$k_3 = \frac{y_3}{(t_3 - t_1)(t_3 - t_2)}$$

The TOF is obtained by subtracting, from t, all the delays introduced by the hardware, the software and the time multiplexing.

2.2 Position Estimation via Data Fusion

The position estimation is based on the TOF data fusion method [9], by combining estimates of the TOF of the MR signal arriving at the four sensors of the Goalkeaper (GK). As we will show, the problem can be solved by linear regression of several measures from the four sensors. Considering that at a room temperature of 22° the speed of sound is $c = 344$ m/s [10], the distance between the MR and each of the elements of the USS array is given by equation (1). By solving the following equation for all sensors:

$$d_i^2 = (x_i - x_m)^2 + (y_i - y_m)^2, \tag{5}$$

where $i = 0, 1, 2, 3$ is the number of the USS, we can estimate the coordinates (x_m, y_m) of the MR. The x coordinates of the four sensors of the array USS are given by

$$x_0 = -0.3,\ x_1 = -0.1,\ x_2 = 0.1,\ x_3 = 0.3,$$

where the distances are in meters. The y coordinate is zero for all sensors.

This simplifies equation 5 which can be rewritten as the following distance equations,

$$d_i^2 = (x_i - x_m)^2 + y_m^2 \tag{6}$$

Subtracting the (6) for $i = 0$, from the same equation for $i = [1 \dots 3]$ we get,

$$\begin{aligned} d_1^2 - d_0^2 &= x_1^2 - x_0^2 - (2x_1 - 2x_0)x_m \\ d_2^2 - d_0^2 &= x_2^2 - x_0^2 - (2x_2 - 2x_0)x_m \\ d_3^2 - d_0^2 &= x_3^2 - x_0^2 - (2x_3 - 2x_0)x_m \end{aligned} \tag{7}$$

By rearranging terms, the above three equations can be written in matrix form as

$$\begin{bmatrix} x_1 - x_0 \\ x_2 - x_0 \\ x_3 - x_0 \end{bmatrix} \begin{bmatrix} x_m \end{bmatrix} = \frac{1}{2} \begin{bmatrix} x_1^2 - x_0^2 - d_1^2 + d_0^2 \\ x_2^2 - x_0^2 - d_2^2 + d_0^2 \\ x_3^2 - x_0^2 - d_3^2 + d_0^2 \end{bmatrix} \tag{8}$$

which can be rewritten as

$$Ax_m = b, \tag{9}$$

where

$$A = \begin{bmatrix} x_1 - x_0 \\ x_2 - x_0 \\ x_3 - x_0 \end{bmatrix}, \quad b = \frac{1}{2} \begin{bmatrix} x_1^2 - x_0^2 - d_1^2 + d_0^2 \\ x_2^2 - x_0^2 - d_2^2 + d_0^2 \\ x_3^2 - x_0^2 - d_3^2 + d_0^2 \end{bmatrix} \tag{10}$$

The solution is given by 11 and is the value that minimises the mean quadratic error. This equation is implemented directly in the DSP, since for every measure A and b are constants.

$$x_m = (A^T A)^{-1} A^T b \tag{11}$$

The y coordinate can be estimated by averaging the four values of y_m,

$$y_m = \sqrt{d_i^2 - (x_i - x_m^2)} \tag{12}$$

which can be approximated by,

$$y_m = \sqrt{d_m^2 - x_m^2}, \tag{13}$$

where d_m is the average of the four $d_i's$. For distances above one meter the error produced by this simplification is less than 3%.

We can use temporal averaging to reduce the robot position estimation error. If we combine N measures then solving the following system of equations

$$\begin{bmatrix} A_0 \\ A_1 \\ \vdots \\ A_{N-1} \end{bmatrix} \begin{bmatrix} x_m \end{bmatrix} = \begin{bmatrix} b_0 \\ b_1 \\ \vdots \\ b_{N-1} \end{bmatrix} \tag{14}$$

produces a position estimation with less error at the expense of dynamic system response to the movement of the robot. To obtain the localization results shown in this work we used $N = 8$.

3 Hardware Prototype

We chose the TMS320F2812 DSP from Texas Instruments to perform the signal processing tasks. This DSP has 16 analog inputs sampled by a high speed ADC. Figure 5 shows a block diagram with the architecture of the acquisition system. The USS are mounted on a circuit board that performs a pre-amplification (gain=30) of the ultrasonic signal followed by bandpass filtering.

The amplitude of the received signal varies with the inverse of the distance between the transmitter and the receiver. To adjust the amplitude of the received signal to the range of the ADC we built a Programable Gain Amplifier (PGA) for each channel. The PGA is software controlled by the DSP.

As we intend to use the system to test different waveforms for the emitted signals we used an eight channel 12 bits DAC. The output amplifier connected to the ultrasonic transmitter delivers 16Vpp.

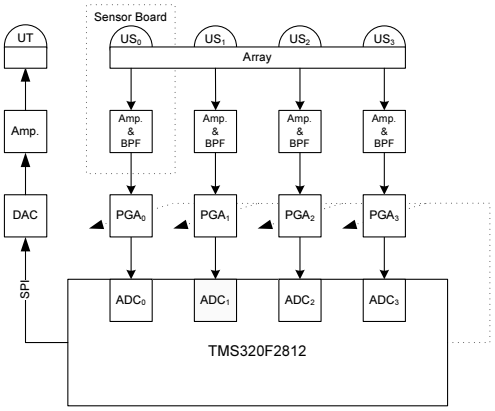

Fig. 5. The goalkeper has an ultrasonic transmitter (UT) to send the broadcast signal and an USS array with four receivers (USS_0 to USS_3). The other robots have four pairs of transmitters/receivers equally spaced around a circle.

Table 1. Anechoic chamber results: θ_r - real angle, θ_m - measured angle, $||\theta_r - \theta_m||$ - absolute error of the measured angle and σ_{θ_m} - standard deviation for each angle.

θ_r	θ_m	$\|\|\theta_r - \theta_m\|\|$	σ_{θ_m}
-90°	-83.63°	6.37°	1.90°
-80°	-69.31°	10.69°	0.21°
-70°	-68.55°	1.45°	0.37°
-60°	-62.27°	2.27°	0.40°
-50°	-36.11°	13.89°	0.22°
-40°	-42.72°	2.72°	1.20°
-30°	-34.95°	4.95°	0.14°
-20°	-19.15°	0.85°	0.31°
-10°	-8.73°	1.27°	0.24°
0°	0.36°	0.36°	0.24°
10°	9.53°	0.47°	0.50°
20°	24.54°	4.54°	0.43°
30°	43.11°	13.11°	0.88°
40°	39.45°	0.55°	0.23°
50°	42.59°	7.41°	0.18°
60°	47.49°	12.51°	0.79°
70°	69.31°	0.69°	0.21°
80°	70.66°	9.34°	0.37°
90°	83.86°	6.14°	2.32°

4 Experimental Results

Anechoic Chamber Tests. To gauge the localization system we tested it on two different situations, in an anechoic chamber and in a robot soccer field. In the anechoic chamber we only tested the angle measurement in the -90° $\leq 0 \leq$ 90° range using 10° intervals with the transmitter at a distance of 7.5m. For each angle we took 5 measures. The results of this test are shown in table 1.

In this experiment we observed that for angles between 30°and 60°the system was very sensitive to small angle variations and that the received signal envelope was double peaked due to multipath interference.

Robot Soccer Field Tests. We also performed localization tests in a robotics soccer field. From this tests we got values for the absolute error position in a 1m grid for half

the field from 0 to -3m in the x coordinate and from 1 to 8m in the y coordinate. For each position 50 measures were taken allowing the calculation of some statistical parameters such as mean and the standard deviation of the measured distance and angle.

A $X-Y$ plot with the test measurements and the estimated mean positions is shown in figure 6.

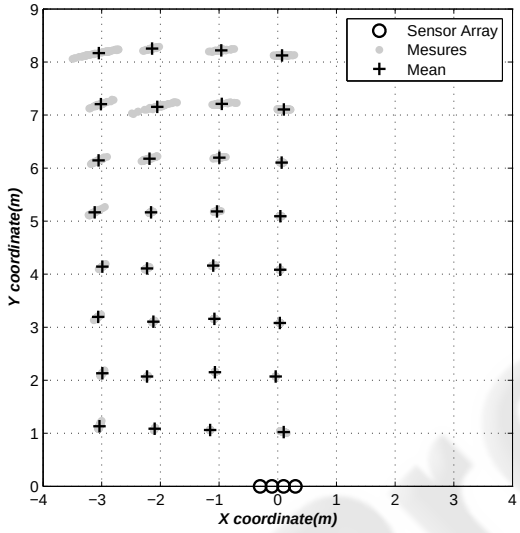

Fig. 6. Position measures obtained in the soccer field with the USS array.

The error associated with the polar coordinates, distance and angle, of a position test are presented in figures 7 a) and b). The distance has a maximum standard deviation $\sigma_{d_m} = 1$cm and the angle has a maximum standard deviation of $\sigma_{\theta_m} = 1,84°$.

From the results shown in figure 6 it is observed that as the distance increases, the variability of the measured position also increases. This can be explained by the degradation of the signal to noise ratio of the received signals as the distance increases.

5 Conclusion

In this work we presented a complete system to localize soccer robots. An ultrasonic sensor array combined with time data fusion, reduced the standard variance of the angle measurements from 10° to 2°.

To improve the signal to noise ratio of the received signal (for large distances) the system transmitted chirp pulses with a duration of 6.4ms. To be able to process the four receiver channels simultaneously with a low cost DSP we implemented an efficient baseband converter.

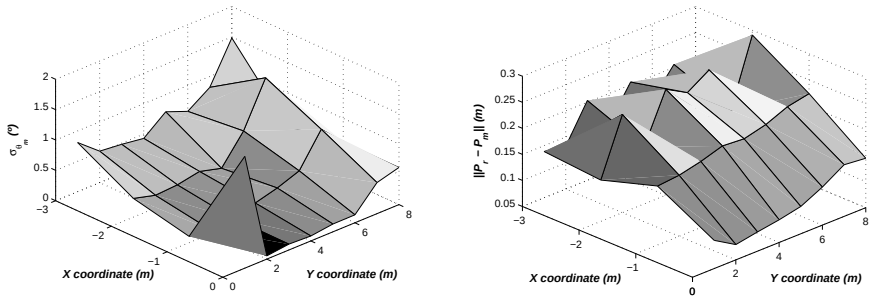

(a) Angle (b) Position

Fig. 7. Standard angle error and absolute position error.

References

1. Moravec, H.P., Elfes, A.: High resolution maps from wide angle sonar. In: Proceedings IEEE International Conference on Robotics and Automation, Washington D. C., IEEE (1985) 116–121
2. Elfes, A.: Sonar-based real world mapping and navigation. IEEE Transactions on Robotics and Automation **4** (1987) 249–265
3. Sabatini, A.M., Spinielli, E.: Correlation techniques for digital time-of-flight measurement by airborne ultrasonic rangefinders. In: Proceendings of the IROS'94, Munich, Germany (1994)
4. Jrg, K.W., Berg, M.: Sophisticated mobile robot sonar sensing with pseudo-random codes. Robotics and Autonomous Systems **25** (1998) 241–251
5. Vieira, J.M., Lopes, Srgio, I., Bastos, C.A.C., Fonseca, P.N.: Sistema de localizao utilizando ultra-sons. In: Robtica 2006, Guimares, Portugal (2006)
6. Cook, C.E., Bernfeld, M.: Radar Signals - An Introduction to Theory and Application. Artech House, Norwood (1993)
7. Sabatini, A.M., Rocchi, A.: Sampled baseband correlators for in-air ultrasonic rangefinders. IEEE Transactions on Industrial Electronics **45** (1998) 341–350
8. Vaidyanathan, P.P.: Multirate Systems and Filter Banks. 1 edn. Signal Processing. Prentice-Hall, New Jersey (1993)
9. Sayed, A.H., Tarighat, A., Khajehnouri, N.: Network-based wireless location. IEEE Signal Processing Magazine **22** (2005) 24–40
10. Kočiš, S., Figura, Z.: Ultrasonic Measurements and Technologies. Sensors Physics and Technology. Chapman & Hall, London, UK (1996)